

Simplified optical payload with digital interferometry

Glenn de Vine,¹ Kirk McKenzie,¹ Brent Ware,¹ Robert E. Spero,¹
William M. Klipstein,¹ Danielle Wuchenich,^{1,2} Daniel A. Shaddock.^{1,2}

1. Jet Propulsion Laboratory,
California Institute of Technology,
4800 Oak Grove Drive, Pasadena, CA, 91109, USA.

2. Centre for Gravitational Physics,
The Australian National University, Canberra, ACT, 0200, Australia.

glenn.devine@jpl.nasa.gov (818-354-5437), kirk.mckenzie@jpl.nasa.gov,
brent.ware@jpl.nasa.gov, spero@jpl.nasa.gov, klipstein@jpl.nasa.gov,
danielle.wuchenich@anu.edu.au, daniel.shaddock@anu.edu.au.

- Instrument Concept; Enabling Technology.

- We are willing to participate and present this concept at the workshop if invited.

November 9, 2011

Document does not contain sensitive or proprietary information. Cleared for
unlimited release, clearance number: **CL#11-5101**

This research was carried out at the Jet Propulsion Laboratory, California Institute
of Technology, under a contract with the National Aeronautics and Space
Administration. ©2011. All rights reserved.

Contents

1	Introduction	1
1.1	Enabling Technology Proposal for a Gravitational Wave Space Mission	1
2	Digital Interferometry for a Gravitational Wave Mission	2
3	Digital Interferometry background	4
4	Experimental demonstrations of Digital Interferometry	6
4.1	DI multiplexing	6
4.2	DI displacement sensitivity	6
4.3	DI with optical demodulation	7
5	Conclusions	8

1 Introduction

We describe the application of digital interferometry (DI) [1] in a laser metrology system for application to a LISA-like gravitational wave (GW) space mission, enabling removal of many components of the optical payload, such as the telescope truss and optical bench, presenting potential drastic complexity and mass savings. While DI is a relatively new technology, many demonstrations have been performed and applications developed. In the 10-20 year timescale likely for a gravitational wave space mission to be developed, the technique will become very mature.

Main concept highlights:

- remove picometre requirements on optical path length stability inside the spacecraft;
- replace massive ultra-low expansion Optical Bench with a compact all-fibre or waveguide system.

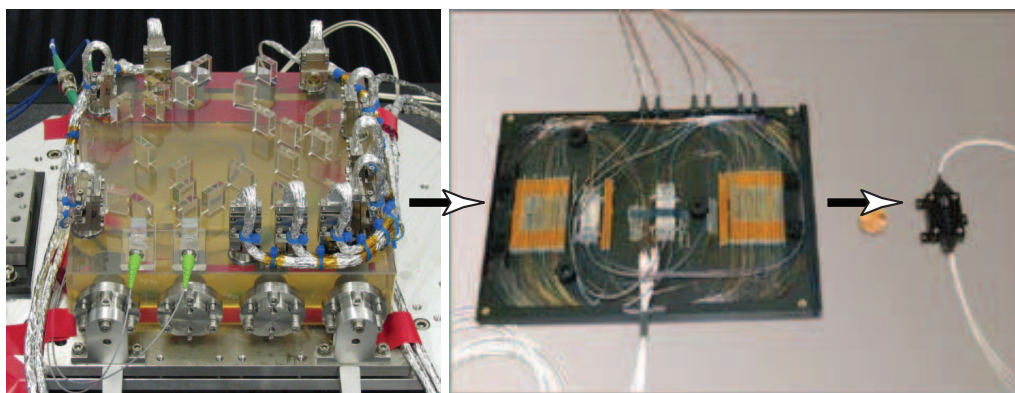


Figure 1: Digital interferometry will remove complexity and mass by negating the need for an optical bench, instead using optical fibers and, in its ultimate form, a photonic integrated circuit.

- the **mass** of our system would be approximately the mass of the present optical subsystem minus that of the large optical bench and its bonded optics;
- removal of the optical bench will save 1-2 years of development **costs** and the actual costs of the 6 benches required, 2 on each spacecraft;
- the **power** consumption would be approximately equal to that presently estimated for LISA;
- overall the DI technique itself is **TRL 4**; the DI phasemeter is TRL 4-5, as is the photoreceiver.

1.1 Enabling Technology Proposal for a Gravitational Wave Space Mission

Digital interferometry has already been employed in a number of proof-of-principle measurements demonstrating its multiplexing and near-picometre performance capabilities (see Section 4). We will construct an experimental testbed based on figure 2, to demonstrate that DI can measure the critical optical path-lengths, with a target of $5 \text{ pm}/\sqrt{\text{Hz}}$ at 3 mHz.

	Displacement Sensitivity [pm/ $\sqrt{\text{Hz}}$]	No. of Targets (Multiplexing)	Minimum Range-gate [cm]
Current Capability	5 (at 1 Hz)	4	3 to 187.5*
GW mission requirement	~ 10 (at 3 mHz)	~ 10	~ 20

Table 1: Comparison of current demonstrated DI capabilities and those required for a GW mission. *An advanced application of DI has measured component separations of 3 cm, while the more traditional method has measured 187.5 cm. An experiment is underway, using the traditional method, capable of measuring optical component separations of 12 cm. See Section 4 for details of each of these.

DI is a laser metrology technique employing pseudo-random noise (PRN) codes phase modulated onto an optical carrier. Combined with heterodyne interferometry, the PRN code is used to select individual signals, returning the inherent interferometric sensitivity determined by the optical wavelength. The signal isolation arises from the autocorrelation properties of the PRN code; enabling both rejection of spurious signals (e.g. from scattered light) and multiplexing capability using a single metrology system. The minimum separation of optical components is determined by the wavelength of the PRN code.

Rather than build the entire payload to be stable at the picometre level, we use advances in optical metrology to simply measure at the pm level. Digitally-enhanced heterodyne interferometry has characteristics that make its application attractive for any laser interferometry space mission, especially those with high path-length stability requirements such as a gravitational wave mission. These characteristics include strong immunity to scattered light, one of the main technical noises sources associated with laser interferometry and metrology, and its inherent multiplexing capabilities, allowing the technique to measure many optics with a single detector. Combined, these properties enable a smaller and lighter payload, with lower optical complexity, for the same noise performance. For example, the LISA baseline design requires passive stability of optical components in the sensitive path of the order of picometers. With digital interferometry, we can remove this requirement and instead rely on the multiplexing capabilities to measure the various path length fluctuations, allowing them to be subtracted in post-processing. This shifts the complexity of the optical bench from the hardware to the digital signal processing.

In our LISA lab at JPL, we have previously shown picometre performance from rigid interferometers and time-delay interferometry (TDI) performance meeting the LISA requirements on the JPL LISA testbed [3]. Much like the LISA testbed, we would build the DI experiment in a similar manner and demonstrate TDI in this experiment. This would give validation to the compatibility of DI with LISA interferometry and TDI. Such an experiment would also ultimately include point ahead angle and wavefront sensing in the DI readout.

2 Digital Interferometry for a Gravitational Wave Mission

The LISA baseline design requires passive stability of optical components in the sensitive path, of the order of picometers on the optical bench. With DI we can remove this requirement and instead rely on DI's multiplexing capabilities to measure path length fluctuations, subtracting them in post-processing. As shown in figure 2, this allows the optical bench subsystem to be implemented almost entirely in optical fibers, with only one or two small optical benches without picometre stability requirements.

DI will subtract the path-length noises in post-processing by making the following measurements:

i. Bench-to-Bench Measurement

Figure 3 shows the optical path between spacecraft and the various path-lengths we will measure using DI to construct a bench-to-bench measurement insensitive to telescope expansion. The left and right-most optics are the fiducial points for the bench-to-bench measurement. The desired bench-to-bench measurement is then:

$$L_0 = L_1 + L_2 + L_3 + L_4 + L_5$$

Actual optical path:

$$M_0 = L_1 + 3L_2 + L_3 + 3L_4 + L_5$$

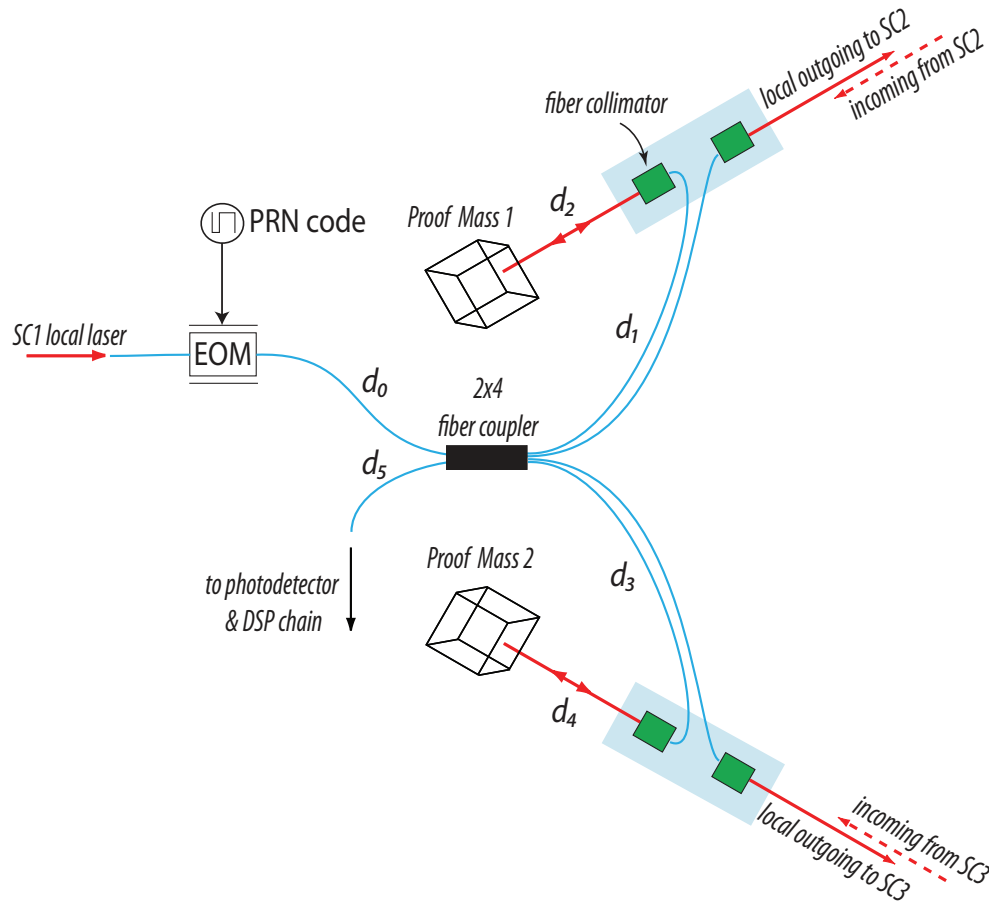


Figure 2: Possible DI measurement scheme on a LISA spacecraft, replacing the optical bench and telescope truss with optical fibers and digital interferometry.

DI will measure (i) the displacement of the first fiducial mirror and (ii) the reflection from the secondary mirror on the left bench. Taking the difference between (i) and (ii) yields:

$$M1 = 2(L_1 + L_2)$$

Backscattered light from the left bench's primary mirror can also be differenced with the fiducial displacement (i) to give:

$$M2 = 2(L_1 + 2L_2)$$

Likewise we construct equivalent measurements on the right bench:

$$M3 = 2(L_5 + L_4) \text{ and } M4 = 2(L_5 + 2L_4)$$

We can form L0 from these measurements:

$$L_0 = M0 - (M2 - M1) - (M4 - M3)$$

Note that even if the telescope mirrors move, we can subtract this out from the bench-to-bench measurement, thereby removing the requirement for picometer stability.

ii. Proof Mass-to-Bench Measurement

As above, we can form a proof mass-to-bench measurement. With reference to figure 2, the desired proof mass-to-bench measurement is:

$$R = d_2$$

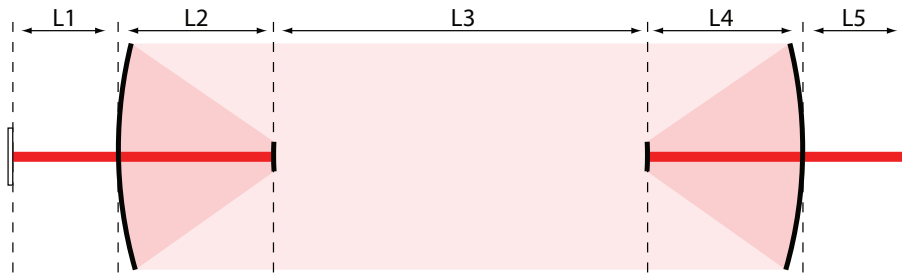


Figure 3: Bench-to-Bench measurement between spacecraft.

Actual optical path:

$$P0 = d_0 + 2(d_1 + d_2) + d_5$$

DI will measure the back-reflection from the collimator:

$$P1 = d_0 + 2d_1 + d_5$$

Thus we form R from these measurements:

$$R = \frac{(P0 - P1)}{2}$$

The designs and calculations above assume the required picometer performance in our DI displacement measurements, including the phasemeter. We have previously developed a phasemeter [2] capable of meeting and exceeding the LISA requirements, including sub-microcycle performance (equating to sub-picometer performance for a laser wavelength of one micron). LISA's current main interferometry challenges (backlink fiber and telescope backscatter) are not issues here. The simplification of the optical bench and removal of the optical truss could allow for a smaller spacecraft and significant cost reductions. Realizing this new metrology architecture allows the optical bench to be implemented in a compact fiber-coupled waveguide.

3 Digital Interferometry background

Table 2 shows the effect of the PRN encoding and decoding on the measured signals corresponding to the accompanying experimental layout (figure 4). The first row shows the signal at the photodetector in a conventional heterodyne interferometer (a beat-note at f_h). In digital interferometry, the PRN code (A) phase modulated onto the light randomly inverts the heterodyne signal at the photodetector producing a chopped sine wave (B). In signal processing the photodetector output is multiplied by the PRN code with a matching delay (C1), to recover the original heterodyne signal (D1). Optical path length information is contained in the phase of this heterodyne signal. The right-hand column shows the signals obtained using a mismatched decoding delay (C2); in this case the signal is randomly re-inverted (D2) and appears in the measurement as a broadband noise floor. This broad spectrum, or white, noise can be strongly rejected by appropriate filtering and averaging in the phasemeter. This demonstrates that by adjusting the decoding delay, we can selectively isolate signals based on their total optical/electronic delay.

Although an acousto-optic modulator, AOM, is shown here, it is more typical to employ a second laser, off-set phase-locked to the first, to create the heterodyne signal. Alternatively, a new variant of DI, called Homodyne DI, removes the heterodyne measurement entirely and instead employs quadrature phase-shift keying (QPSK), which modulates the pseudo-random code with four phases

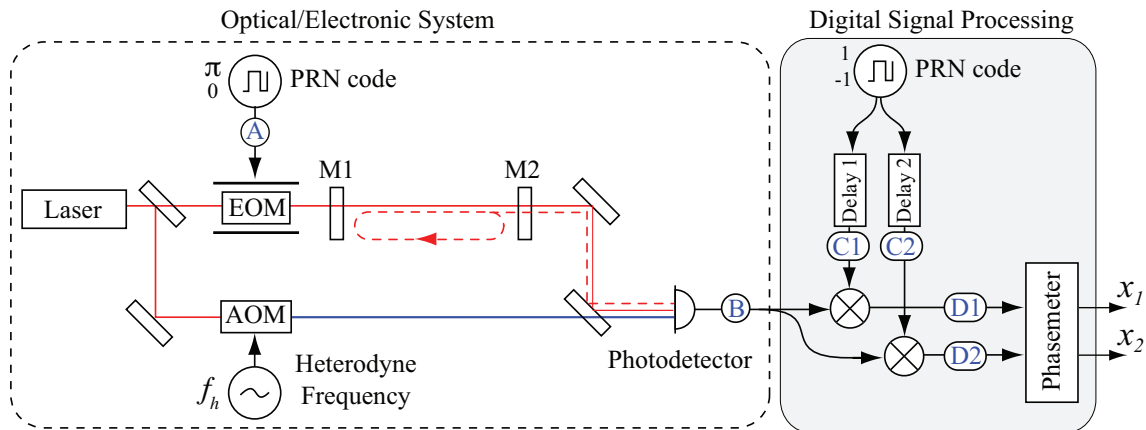


Figure 4: Digital Interferometer for monitoring displacements of two mirrors, M1 and M2. Signals are isolated by matching the decoding delays to the optical delays. Signals measured at points A, B, C1, C2, D1, and D2 are shown in Table 2.

	Matched decoding delay	Mismatched decoding delay
Conventional heterodyne		
PRN encoding	(A) 0 π	(A)
Detected single-pass signal	(B)	(B)
PRN decoding	(C1) 1 -1	(C2)
Decoded output	(D1)	(D2)

Table 2: Signals from single-pass beam with matched (middle column) and unmatched (right column) decoding delays. Signals A, B, C1, C2, D1, D2 correspond to the measurement points in fig. 4.

(0° , 90° , 180° and 270°), instead of two (0° and 180°). Homodyne or QPSK DI has recently been demonstrated, achieving displacement noise levels of around $100 \text{ pm}/\sqrt{\text{Hz}}$ at 1 Hz [4].

The shot noise level of DI is equivalent to the shot noise level of conventional heterodyne interferometry. Like other broadband noise (e.g. electronic noise), the shot noise level is unaffected by the digital decoding due to the random nature of shot noise and its lack of correlation with the PRN code. The single sided amplitude spectral density of phase noise due to shot noise for each decoded output is given by,

$$\delta\phi_{SN} = \sqrt{\frac{h\nu}{P}} \text{ rad}/\sqrt{\text{Hz}}. \quad (1)$$

where P is the detected optical power of the signal, h and ν Planck's constant and the optical frequency respectively. For round-trip measurements this can be converted to displacement noise by multiplying by $\lambda/4\pi$ (or $\lambda/2\pi$ for one-way measurements). Conventional heterodyne interferometry measurements are often limited by technical noise sources, such as spurious interference, well above the shot noise limit.

4 Experimental demonstrations of Digital Interferometry

DI has shown: the capability to measure multiple optical components with a single detector [5, 6]; high measurement linearity with sub-nanometer cyclic error [7]; and a displacement sensitivity of better than $5 \text{ pm}/\sqrt{\text{Hz}}$ at 1 Hz [8]. DI has been successfully employed to measure component separations from several metres, down to a few centimetres [5].

4.1 DI multiplexing

Three PZT-mounted optics separated by 3.75 metres were driven with the separate signals, as shown in figure 5. The separate signals were recovered by DI by demodulating the signal from the photoreceiver with appropriately delayed PRN codes. Figure 6 shows the results of the multiplexing capability of DI.

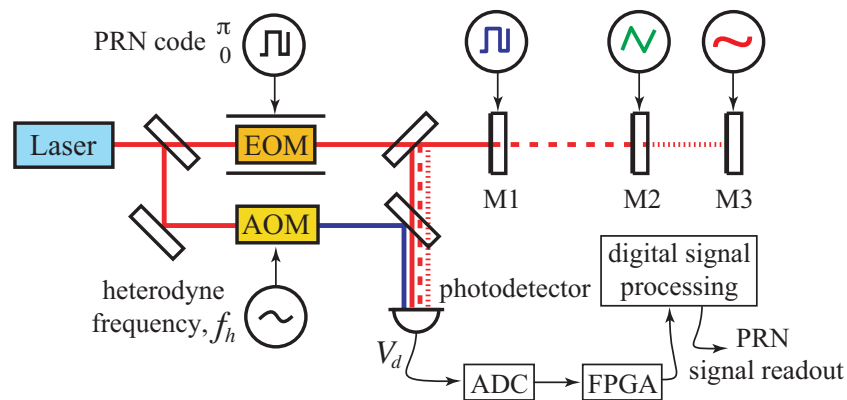


Figure 5: Simplified schematic for DI multiplexing experiment.

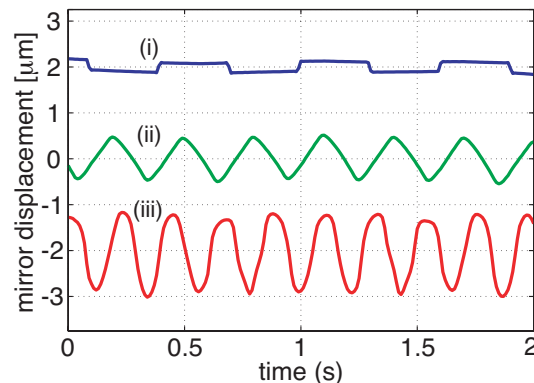


Figure 6: Experimental multiplexing results obtained by driving three PZT-mounted optics with the signals shown, each separated by 3.75 m.

4.2 DI displacement sensitivity

Figure 7 shows the root power spectral density of a DI displacement measurement of a 3.75 m linear cavity locked with the PDH technique. This measurement was made using the 2nd and 6th round-trip beams on transmission through the cavity. A displacement sensitivity of better than $5 \text{ pm}/\sqrt{\text{Hz}}$ was achieved at a few Hertz.

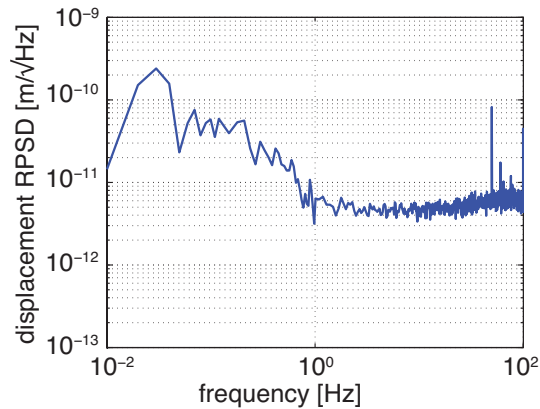


Figure 7: Spectral density of the DI measurement of cavity displacement when the cavity is locked using PDH locking. Spectral density averaged for clarity ($3\times$ for $0.1 > f > 1$ Hz, $10\times$ for $f > 1$ Hz).

4.3 DI with optical demodulation

The DI demonstrations presented thus far required optical component separations of several meters (set by the wavelength of the PRN code employed, 80 MHz equating to 3.75 m, and limited by digital processing speed). An experiment currently under way is employing electronics capable of processing 1.25 GHz signals, equating to a length of 0.24 m, enabling component separations of 0.12 m to be measured. However, a variation of DI, employing optical demodulation, enables measurements of optical components only a few centimeters apart. Instead of the usual electronic decoding, the DI signal is interfered with an appropriately delayed, identically PRN encoded, local oscillator beam. Optical decoding also allows the use of a low-bandwidth signal processing chain with GHz codes, negating the need for high-speed detectors and digital signal processing. This reduced bandwidth also reduces the power consumption of the entire system.

Figure 8 presents a simplified experimental layout used for the demonstration of optical demodulation with DI. The heterodyne signal is created by off-set phase-locking two lasers with a digital phase-locked loop at 4 MHz. The error-point is monitored on PD_{DPLL} . PRN codes are phase-modulated by waveguide modulators onto each laser beam. These are subsequently interfered via a fibre beam-splitter, thus optically demodulating the laser signals, before being detected on PD_{signal} .

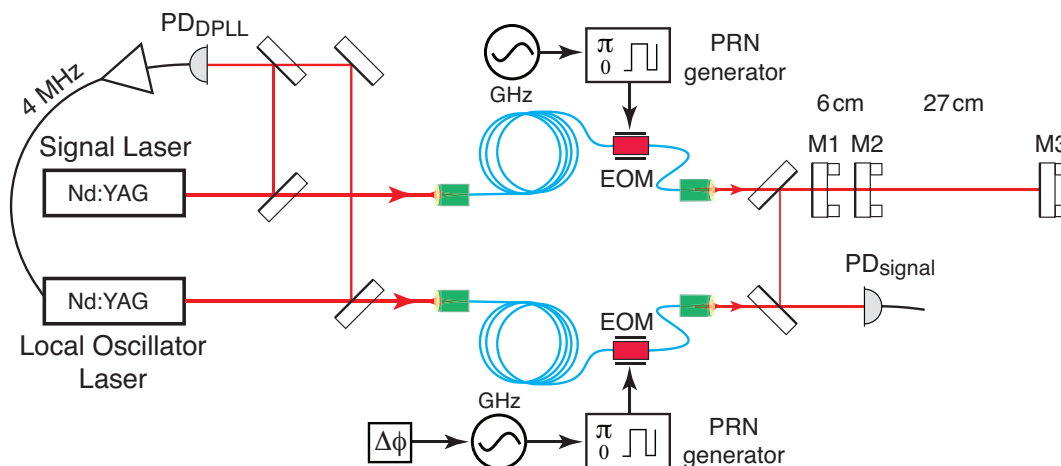


Figure 8: Simplified experimental schematic for DI with optical demodulation of GHz codes.

The results are shown in time and frequency in figure 9. The green traces show the 4 MHz heterodyne beat-note with no PRN encoding. The red traces show when the codes are not aligned in phase. Some residual 4 MHz beat-note can be seen in the frequency domain, ~ 50 dB down, compared to the other traces. The blue traces show the recovery of the 4 MHz beat-note after successful optical demodulation.

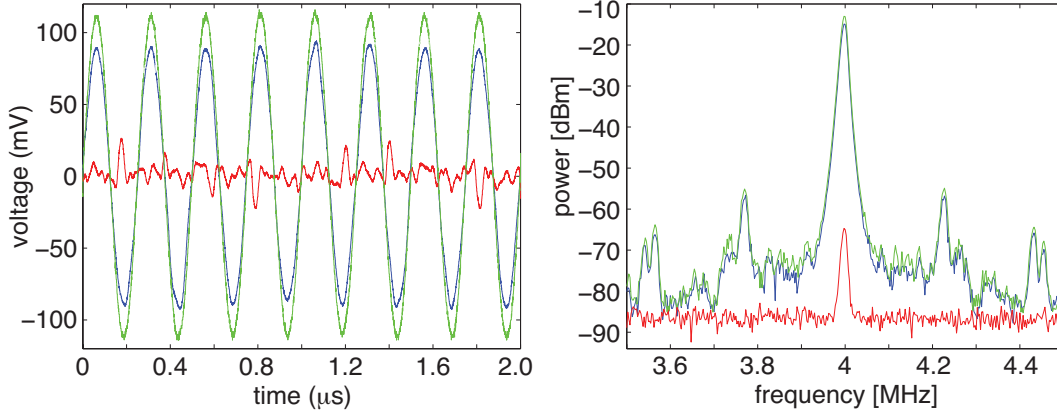


Figure 9: Experimental results for DI with optical demodulation of GHz codes.

Figure 10 shows time-domain traces obtained by scanning the phase of the local oscillator PRN code, presented from oscilloscope data for both 5 GHz and 1 GHz PRN code frequencies. It can be seen that the 5 GHz code (6 cm wavelength) can isolate all three mirrors, however, the 1 GHz code (30 cm) cannot distinguish between mirrors M1 and M2, spaced only 6 cm apart. The final trace, on the right, shows a zero-span RF spectrum analyser scan corresponding with the data of the oscilloscope trace at 5 GHz. A multi-pass reflection has also been detected.

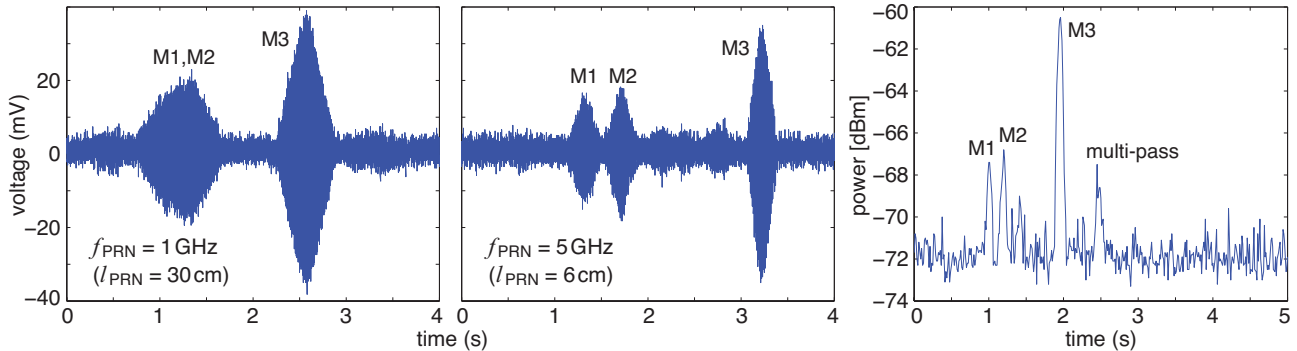


Figure 10: Experimental results from scanning the phase of the local oscillator PRN code, for different code frequencies. It can be seen that the higher code frequency allows measurement isolation of closer optical components.

5 Conclusions

We will construct a testbed to demonstrate that digital interferometry can measure the critical optical path-lengths and meet the performance levels required for a gravitational wave mission. Digital interferometry will greatly reduce the mass and complexity of the optical subsystem onboard LISA or a LISA-like mission. Implementing DI will allow the removal of the optical bench and telescope

truss, and the associated picometre levels of stability required for these systems. The simplification of the optical bench and removal of the optical truss will allow for a smaller spacecraft and possibly significant cost reductions. Realizing this new metrology architecture would allow the optical bench to be implemented in a compact fiber-coupled waveguide. DI provides immunity to scattered light and electronic crosstalk. Requiring only a single processing chain affords common-mode rejection of electronic phase delays within the signal processing chain. These phase delays currently set a performance limit on the LISA measurement chain at low frequencies. DI is compatible with both heterodyne interferometry, for interspacecraft measurements, and homodyne measurement, for local spacecraft measurements. DI has been employed in proof-of-principle measurements demonstrating its multiplexing and near-picometre performance capabilities.

References and Citations

- [1] D.A. Shaddock, “Digitally Enhanced Heterodyne Interferometer,” *Opt. Lett.* **32**, (2007).
- [2] D.A. Shaddock, B. Ware, P.G. Halverson, R.E. Spero and W. Klipstein, “Overview of the LISA phasemeter,” *AIP Conf. Proc.*, **873**, 654–660, (2006).
- [3] G. de Vine, B. Ware, K. McKenzie, R. E. Spero, W. M. Klipstein, and D. A. Shaddock, “Experimental Demonstration of Time-Delay Interferometry for the Laser Interferometer Space Antenna,” *Phys. Rev. Lett.* **104**, 211103 (2010).
- [4] D.A. Shaddock, A. Sutton, D. Wuchenich, T. Lam, “Digital Enhanced Homodyne Interferometry for High Precision Metrology”, International Quantum Electronics Conference (IQEC) and Conference on Lasers and Electro-Optics (CLEO) Pacific Rim, Sydney, NSW, Australia, August (2011).
- [5] G. de Vine, et al., “Digitally-enhanced heterodyne interferometry with GHz optical demodulation”, 8th Edoardo Amaldi Conference on Gravitational Waves, New York, New York, USA, June (2009).
- [6] D. Wuchenich, et al., “Laser frequency noise immunity in multiplexed displacement sensing”, *Opt. Lett.*, **36**, 672-674, (2011).
- [7] O. Lay, S. Dubovitsky, D. A. Shaddock, and B. Ware, “Coherent range-gated laser distance metrology with compact optical head,” *Opt. Lett.* **32**, 2933-2935 (2007).
- [8] G. de Vine et al, “Picometer level displacement metrology with digitally enhanced heterodyne interferometry,” *Opt. Express* **17**, 828-837 (2009).